MONTE CARLO SIMULATION OF ELECTROMAGNETIC SCATTERING FROM TWO-DIMENSIONAL RANDOM ROUGH SURFACES †

R.L. Wagner, J.M. Song, and W.C. Chew

Center for Computational Electromagnetics
Department of Electrical and Computer Engineering
University of Illinois
Urbana, IL 61801-2991

Abstract

The fast multipole method-fast Fourier transform (FMM-FFT) method is developed to compute the scattering of an electromagnetic wave from a two-dimensional rough surface. The resulting algorithm computes a matrix-vector multiply in $O(N\log N)$ operations. This algorithm is shown to be more efficient than another $O(N\log N)$ algorithm, the multi-level fast multipole algorithm (MLFMA), for surfaces of small height. For surfaces with larger roughness, the MLFMA is found to be more efficient. Using the MLFMA, Monte Carlo simulations are carried out to compute the statistical properties of the electromagnetic scattering from two-dimensional random rough surfaces using a workstation. For the rougher surface, backscattering enhancement is clearly observable as a pronounced peak, in the backscattering direction, of the computed bistatic scattering coefficient. For the smoother surface, the Monte Carlo results compare well with the results of the approximate Kirchhoff theory.

† This work was supported by the Office of Naval Research under grant N00014-95-1-0872, the National Science Foundation under grant NSF ECS 93-02145, and the Army Research Office under grant DAAH04-93-G-0430.

File:paper4a.tex, Date:July 16, 1996.

1. Introduction

The problem of calculating the statistical properties of electromagnetic scattering from random rough surfaces has received considerable attention in recent years. This topic is of interest in fields such as surface physics, satellite remote sensing, and radar data interpretation, where electromagnetic waves interact with surfaces that are rough on the scale of the electromagnetic wavelength. As described by Ishimaru [1]-[2], one of the most interesting phenomena associated with rough-surface scattering (as well as with scattering from other types of random media) is the occurrence of backscattering enhancement. This term describes the appearance of a well-defined peak, in the backscattering direction, of the intensity of the incoherently scattered component of the electromagnetic field. An interesting example is the full moon; as may be observed with the naked eye, the moon is brighter at full moon than at other times. Several approaches have been used to study scattering from rough surfaces. These include approximate analytical methods, experimental studies, and numerical simulations.

The book by Kong [3] provides an introduction to some approximate analytical approaches for studying rough-surface scattering. Two approaches, the Kirchhoff approximation and the small perturbation method, are discussed in this text. Many authors have contributed to the development of approximate analytical theories for rough-surface scattering [4]-[14].

Significant experimental work has also been carried out on rough-surface scattering. See, for example, [15]-[18]. Quite recently, researchers have reported controlled laboratory millimeter-wave experiments on rough-surface scattering [19]-[20].

Because of the limited region of validity (in terms of surface-roughness parameters) of the approximate analytical approaches mentioned above, much work has been done using Monte Carlo simulation in conjunction with rigorous computational electromagnetic simulation techniques. In this approach, a set of random rough surfaces, each with the same statistical roughness properties (surface height distribution and transverse correlation function), is generated. Then the scattering from each surface is computed independently, using an appropriate numerical simulation technique. Finally, the results are processed to determine the statistical properties of the scattered field. This technique has been applied to one-dimensional problems [21]-[27], two-dimensional scalar wave problems [28]-[31], and two-dimensional vector wave problems [20],[32]-[35]. Note that a two-dimensional problem refers to a problem in which the rough surface is two-dimensional (i.e., the surface height varies as a function of two transverse dimensions); the corresponding electromagnetic scattering problem is a full three-dimensional vector wave problem.

The three-dimensional vector wave scattering problem presents a great computational challenge. Even moderately sized problems can require a very large number of unknowns. In the work that follows, rough surfaces are modeled using the method of moments (MOM). A finite sized rough surface, with edge length L, is illuminated with a Gaussian beam of half-width W. Ideally, W should satisfy $W \gg \lambda$ in order to produce a beam that propagates with a planar wavefront and minimal angular spreading. We also require $L \gg W$ to avoid unwanted edge effects.

Thus, the computational requirements for this problem are very large. Consider, for example, a rough-surface model with edge length $L = 9.15\lambda$, where λ is the radiation wavelength. If the problem is discretized with seven unknowns per wavelength in the mean plane of the surface, the number of surface current unknowns is $N = 8096$. The memory required to store the MOM matrix for this problem is 520MB (assuming the use of single-precision arithmetic). The estimated CPU time (on a SUN SPARC-10 workstation) required to fill the MOM matrix is approximately 12 hr. The estimated time for a direct solution of the matrix equation, using LU decomposition, is approximately 50 hr. If an iterative solution scheme is used, each matrix-vector multiply will take approximately 2 min. Considering that many realizations of the random rough surface must be computed for Monte Carlo simulation (typically around 100 or more realizations), the costs of a brute force solution are unacceptable. In the absence of a much more powerful computer, efficient computational strategies must be employed to obtain a solution.

This paper describes our efforts to address this demanding problem. Our goal is to solve large-scale random rough-surface scattering problems using an MOM/Monte Carlo approach, utilizing efficient solution strategies to reduce the computational requirements. We also wish to search for interesting physical phenomena associated with rough-surface scattering, particularly backscattering enhancement.

2. Model Development

In this work, perfectly conducting Gaussian random surfaces are considered. The surface is defined by a surface height function $z(\mathbf{r}_s)$, where $\mathbf{r}_s = (x, y)$. The statistical characteristics of the Gaussian rough surface are defined by the properties

$$\langle z(\mathbf{r}_s)\rangle = 0, \tag{1}$$

$$\langle z(\mathbf{r}_s)z(\mathbf{r}'_s)\rangle = \sigma^2 e^{-|\mathbf{r}_s-\mathbf{r}'_s|^2/l^2}. \tag{2}$$

In the above equations, the angular brackets denote the average over the ensemble of realizations. The parameter σ is the RMS surface height, and l is the transverse correlation length.

Random surfaces with these properties are generated using essentially the procedure outlined in Garcia and Stoll [22]. First, working on a discrete mesh of points in the x-y plane, an uncorrelated Gaussian random surface distribution $z_u(\mathbf{r}_s)$ is generated. This step is easily accomplished using any Gaussian random number generator. This surface has the properties

$$\langle z_u(\mathbf{r}_s)\rangle = 0, \tag{3}$$

$$\langle z_u(\mathbf{r}_s)z_u(\mathbf{r}'_s)\rangle = \sigma^2 \delta(\mathbf{r}_s - \mathbf{r}'_s). \tag{4}$$

To obtain the desired Gaussian correlation function, this surface must be convolved with a Gaussian filter

$$F(\mathbf{r}_s) = \frac{1}{\sqrt{\pi}(\frac{l}{2})} e^{-|\mathbf{r}_s|^2/(l^2/2)}. \tag{5}$$

That is, set

$$z_c(\mathbf{r}_s) = \iint_{-\infty}^{\infty} F(\mathbf{r}_s - \mathbf{r}'_s) \times z_u(\mathbf{r}'_s)\ d\mathbf{r}'_s. \tag{6}$$

In practice, this convolution is implemented by the fast Fourier transform (FFT) using the discrete grid of surface points mentioned above. It is readily verified, using Equations (3) through (6), that z_c satisfies the defining equations for a Gaussian random surface, Equations (1) and (2). In the work that follows, the edge length (in the x-y plane) of the rough surface will be denoted by L.

In order to limit the area of the rough surface that is illuminated and, hence, avoid unwanted edge effects (since we wish to model scattering from an infinite surface), a Gaussian beam is used for the incident field. In constructing this beam, we follow Tran and Maradudin [33] and use a summation of plane waves

$$\mathbf{E}^{inc}(\mathbf{r}) = \frac{2\pi W^2}{L^2} \sum_{|\mathbf{K}|\le k_0} \hat{\mathbf{e}}^{\mathrm{inc}}(\mathbf{K}) \exp(i\mathbf{K}\cdot\mathbf{r}_s) \exp(-ik_z z) \exp[-(\mathbf{K}-\mathbf{K}_0)^2 W^2/2], \tag{7}$$

where

$$\hat{\mathbf{e}}^{\mathrm{inc}}(K_x, K_y, k_z) = \frac{1}{\sqrt{K_x^2 + k_z^2}}[k_z, 0, K_x]. \tag{8}$$

In the above equations, $\mathbf{K}_0$ is the projection of the central wave vector of the incident beam onto the x-y plane; it is assumed to be in the x direction so that $\mathbf{K}_0 = (K_{0x}, 0)$. The edge length of the rough surface is L. In the $z = 0$ plane this beam has a Gaussian shape with half-width W, centered at $\mathbf{r}_s = 0$. The summation over $\mathbf{K} = (K_x, K_y)$ is evaluated numerically, with K_x and K_y being multiples of $2\pi/L$. For each transverse wavenumber $\mathbf{K}$, k_z is determined by the dispersion relation ($K_x^2 + K_y^2 + k_z^2 = k_0^2$), where $k_0 = \omega/c$ is the free space wavenumber. For Equation (7) to represent a downward propagating beam (propagating in the $-z$ direction), the solution to the dispersion relation with $k_z > 0$ is chosen (time dependence $e^{-i\omega t}$ is assumed). The polarization vector $\hat{\mathbf{e}}$ is in the x-z plane; the beam is thus vertically polarized (i.e. TM_z or p polarized). The angle of incidence of the beam is ($\theta = \sin^{-1}(K_{0x}/k_0), \phi = 0$).

Figure 1 shows the magnitude of a normally incident beam plotted in gray-scale on a typical rough surface. At each point on the surface, the shading represents the field magnitude at that point. The surface shown here has edge length $L = 9.15\lambda$ and roughness parameters $\sigma = 0.7\lambda$ (RMS surface height) and $l = 1.5\lambda$ (transverse correlation length). The beam half-width is $W = 2.3\lambda$. As seen, the resulting spot diameter in the x-y plane is approximately $2 \times W$, or 4.6λ. All distances are in terms of the radiation wavelength, $\lambda = 2\pi/k_0$. Note that W is chosen to be $W \approx L/4$ in order to produce a beam that fits inside the $L \times L$ square surface with minimal edge effects.

Ideally, W should satisfy $W \gg \lambda$ in order to produce a beam that propagates with a planar wavefront and minimal angular spreading. However, this requires large L, which means a larger problem must be modeled. Our choice of computational parameters is based on the trade-off between the desirability of a large beamwidth versus the computational difficulty of modeling the scattering from a larger rough surface. The parameters $L = 9.15\lambda$ and $W = 2.3\lambda$ are used to generate the Monte Carlo results in the next section.

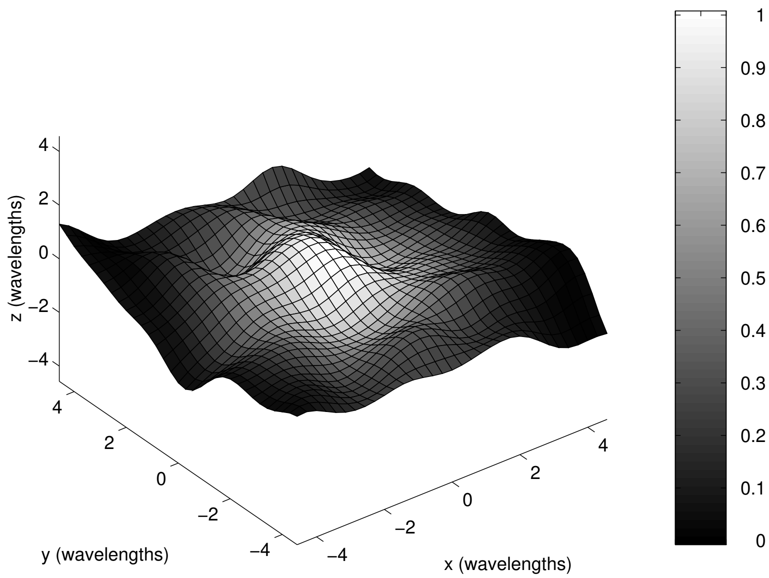

Figure 1. Magnitude of a Gaussian beam (Equation (7)) normally incident on a rough surface with roughness parameters $\sigma = 0.7\lambda$ and $l = 1.5\lambda$. The surface has edge length $L = 9.15\lambda$, and the beam half-width is $W \approx L/4 \approx 2.3\lambda$.

A final issue to consider in developing a rough-surface scattering model is the choice of surface roughness parameters, σ and l. Because one of our goals is to observe the phenomenon of backscattering enhancement, we will focus on σ and l in the range where this is expected to be observed. As discussed in [1]-[2], there are two distinct cases in which backscattering enhancement occurs.

One case involves rough surfaces with RMS height much smaller than a wavelength, where the interface supports a surface wave. This is encountered, for example, in the scattering of light from a rough metal interface. At certain frequencies the metal behaves like a plasma and incident light can excite a surface wave called a "surface plasmon mode" [36] or "surface plasmon polariton" [10]-[14],[37]. The existence of backscattering enhancement in this case is related to the topic of "Anderson localization" [2],[38]. Anderson localization is a multiple scattering phenomenon observed in several physical systems involving random media, including electron transport in strongly disordered material and photon localization in disordered dielectrics. In both of these cases, the localization or enhancement is linked to the presence of "coherent backscattering," the constructive interference of two waves traversing the same scattering path in opposite directions [2].

The other case in which backscattering enhancement is observed occurs when the RMS surface height is close to a wavelength, and the slope is close to one [2]. This case, which is difficult to model using approximate analytical theories, shall be investigated in this work. In this case, the enhancement is also linked to the occurrence of coherent backscattering. This is described by Ishimaru [1]-[2]. Figure 4 in [2] delineates the range of surface roughness parameters for which the different types of backscattering enhancement occur; this served as our guide for choosing σ and l for our numerical experiments.

3. Problem Formulation

The problem to be solved has been defined in Section 2. We wish to compute the scattering of a Gaussian beam from a perfectly conducting rough surface generated using the random surface generator described in Section 2.

Based on the fact that the total (incident plus scattered) tangential electric field must vanish on the conducting surface, we may write the electric field integral equation (EFIE) for the unknown surface current density $\mathbf{J}$. For a conducting surface S, the EFIE is given by [39]

$$\hat{t} \cdot \int_S \left[\mathbf{J}(\mathbf{r}') + \frac{1}{k_0^2} \nabla' \cdot \mathbf{J}(\mathbf{r}') \nabla \right] \frac{e^{ik_0 R}}{R} dS' = \frac{4\pi i}{k_0 \eta_0} \hat{t} \cdot \mathbf{E}^{inc}(\mathbf{r}), \qquad \mathbf{r} \in S. \tag{9}$$

In the above equation, $\hat{t}$ is any unit tangent vector on S, k_0 is the free-space wavenumber, η_0 is the impedance of free space, $\mathbf{E}^{inc}$ is the incident electric field, and $R = |\mathbf{r} - \mathbf{r}'|$.

The above equation is solved using a moment method solution with a parametric geometry description. In this approach, the surface is divided into a set of connected quadrilateral patches, with each patch being determined by a three by three grid of points. For the rough surfaces modeled here, these nine points are taken from the discrete mesh described in Section 2. Each patch is represented mathematically as a parametric quadratic surface. Thus, the vector from the origin to the surface of the p-th patch may be written as

$$\mathbf{r}_p(u_1, u_2) = \sum_{m=1}^{3}\sum_{n=1}^{3} \mathbf{C}_{mn}^{(p)} u_1^{m-1} u_2^{n-1}, \tag{10}$$

where u_1 and u_2 vary from 0 to 1 and $\mathbf{C}_{mn}^{(p)}$ are the vector coefficients of the parametric expansion and are determined from the nine known points on the patch.

To represent the surface current $\mathbf{J}$, each patch is segmented into quadrilateral cells, which are rectangular in parametric space. The current is then expanded in a set of N generalized rooftop basis functions $\{\mathbf{j}_n\}$ that straddle each pair of adjacent cells. These basis functions are similar to planar rooftop basis functions but contain metric factors that account for the surface curvature and guarantee the continuity of the normal component of the surface current flowing along each basis function [39]. These basis functions are the extensions to quadrilateral patches of the curved triangular basis functions of [40], which, in turn, represent the extension to curved surfaces of the flat triangular basis functions of Rao, Wilton, and Glisson [41].

The testing functions used here are constant along the line joining the centers of two adjacent cells. This is called "line matching," and has been found to produce the same accuracy as Galerkin's method (in which the testing and basis functions are identical). Denoting the set of N testing functions by $\{\mathbf{t}_m\}$, the MOM matrix equation may be written as

$$\mathbf{Z} \cdot \mathbf{j} = \mathbf{e}, \tag{11}$$

where $\mathbf{Z}$ is the dense $N \times N$ impedance matrix with elements

$$Z_{mn} = \int_S dS\ \mathbf{t}_m(\mathbf{r}) \cdot \int_S dS' \left[\mathbf{j}_n(\mathbf{r}') + \frac{1}{k_0^2}\nabla' \cdot \mathbf{j}_n(\mathbf{r}')\nabla\right] \frac{e^{ik_0R}}{R}, \tag{12}$$

and $\mathbf{e}$ is a vector of length N, with elements

$$e_m = \frac{4\pi i}{k_0\eta_0} \int_S dS\ \mathbf{t}_m(\mathbf{r}) \cdot \mathbf{E}^{inc}(\mathbf{r}). \tag{13}$$

Once Equation (11) is solved for the surface current, the scattered field may be computed by integration. The results obtained by this method compare well with other computed, analytical, and measured results [39]. To attain a given solution accuracy, this approach has been shown to require fewer unknowns than a flat patch surface model, because of the more accurate geometry modeling provided by the curved patches.

Note that the computed quantity of interest here is the incoherent part of the bistatic scattering coefficient. This scattering coefficient is simply the RCS of the rough surface, normalized by the total incident power [3]

$$\gamma_{ab}^{r}(\hat{k}_s, \hat{k}_i) = \frac{4\pi r^2 (S_r)_a}{P^{inc}} \qquad (a, b = V, H). \tag{14}$$

In the above, a represents the polarization of the scattered wave, either vertical (V) or horizontal (H), and b represents the polarization of the incident wave. The vectors $\hat{k}_i$ and $\hat{k}_s$ are the incident and scattered field propagation directions. $(S_r)_a$ is the polarization-dependent power density in the scattered wave. For example, if the far-zone scattered field is given by

$$\mathbf{E}^{scat}(\hat{k}_s) = \frac{e^{ik_0 r}}{r} \left(\hat{\theta} e_V^{scat}(\hat{k}_s), \hat{\phi} e_H^{scat}(\hat{k}_s) \right) \tag{15}$$

then the scattered power density in polarization a is

$$(S_r)_a = \frac{|e_a^{scat}(\hat{k}_s)|^2}{2\eta_0 r^2}. \tag{16}$$

P^{inc} is the total power incident upon the rough surface. For the Gaussian beam of Equation (7), the total incident power is the sum of the power in each plane wave

$$P^{inc} = \frac{L^2}{2\eta_0} \times \frac{4\pi^2 W^4}{L^4} \sum_{|\mathbf{K}| \leq k_0} \exp\left[-(\mathbf{K} - \mathbf{K}_0)^2 W^2\right] \cos(\theta_{\mathbf{K}}), \tag{17}$$

where $\theta_{\mathbf{K}}$ is the angle of incidence of each plane wave.

The incoherent part of γ is obtained by splitting the scattered field into a mean field and a fluctuating part,

$$\mathbf{E}^{scat}(\hat{k}_s) = \mathbf{E}_m^{scat}(\hat{k}_s) + \mathbf{E}_f^{scat}(\hat{k}_s), \tag{18}$$

where

$$\mathbf{E}_m^{scat}(\hat{k}_s) = \left\langle \mathbf{E}^{scat}(\hat{k}_s) \right\rangle. \tag{19}$$

The angular brackets denote the average over the ensemble of realizations. The scattered intensity is then the sum of coherent and incoherent parts, with the incoherent part being given by

$$\left\langle |\mathbf{E}_f^{scat}(\hat{k}_s)|^2 \right\rangle = \left\langle |\mathbf{E}^{scat}(\hat{k}_s) - \mathbf{E}_m^{scat}(\hat{k}_s)|^2 \right\rangle = \left\langle |\mathbf{E}^{scat}(\hat{k}_s)|^2 \right\rangle - |\mathbf{E}_m^{scat}(\hat{k}_s)|^2. \tag{20}$$

Thus, the incoherent intensity is simply the statistical variance of the scattered field computed over the set of surface realizations. The incoherent part of γ is computed by using the incoherent intensity in computing the scattered power density in Equation (16).

4. An FMM-FFT Algorithm for Rough-Surface Scattering

This section presents a new algorithm developed for the efficient solution of the MOM matrix equation associated with the rough-surface scattering problem. The fast multipole method (FMM) [42]-[56] provides a very efficient and robust method for solving the MOM matrix equation. The FMM is a technique for fast computation of a matrix-vector multiply and is used in conjunction with an iterative matrix solver such as the conjugate-gradient (CG) method. The application of this method to electromagnetic problems is addressed in [42]-[56]. Here we present a modification of the FMM designed to take advantage of the special geometry of the rough-surface scattering problem, in which the scatterer is nearly planar.

A detailed physical description of the FMM is given in the literature [42]-[52]. In the FMM, current elements on the scatterer are grouped together in groups of size M. The matrix elements for the interaction between groups that are near neighbors are calculated using Equation (12) directly. The matrix elements for the interaction between groups that are far away can be expressed as:

$$Z_{mn} = \frac{ik}{4\pi} \int d^2\hat{k} \mathbf{V}_{flm}(\hat{k}) \cdot T_{ll'}(\hat{k} \cdot \hat{r}_{ll'}) \mathbf{V}^*_{sl'n}(\hat{k}), \tag{21}$$

where plane-wave expansions $\mathbf{V}_{flm}(\hat{k})$, $\mathbf{V}^*_{sl'n}(\hat{k})$, and translation matrix $T_{ll'}(\hat{k} \cdot \hat{r}_{ll'})$ are given in [45] and [52], and $\mathbf{r}_l$ and $\mathbf{r}_{l'}$ are the centers of the l-th and l'-th groups, that $\mathbf{r}_m$ and $\mathbf{r}_n$ are belong to, respectively. When we use an iterative method to solve the matrix equations (11), a matrix-vector multiply is to be computed in each iteration. Then, we can write the matrix-vector multiply as

$$\sum_{n=1}^{N} Z_{mn} j_n = \sum_{l' \in B_l} \sum_{n \in G_{l'}} Z_{mn} j_n + \frac{ik}{4\pi} \int d^2\hat{k} \mathbf{V}_{flm}(\hat{k}) \cdot \sum_{l' \notin B_l} T_{ll'}(\hat{k} \cdot \hat{r}_{ll'}) \sum_{n \in G_{l'}} \mathbf{V}^*_{sl'n}(\hat{k}) j_n \tag{22}$$

for $m \in G_l$, where G_l denotes all elements in the l-th group, and B_l denotes all nearby groups of the l-th group (including itself). The first term in (22) is the contribution from the nearby groups, and the second term is the far interaction calculated by FMM. The summation over $n \in G_{l'}$ in the second term of (22) computes the far-field radiation pattern of each group, tabulated at a discrete set of K directions around the unit sphere. For a convergent field expansion, $K = 2(k_0 D + \ln(\pi + k_0 D))^2$, where D is the maximum diameter of a group [52]. Since M is proportional to D^2 for a surface scatterer, M and K are roughly proportional to one another.

The matrix $\mathbf{T}$ translates the K radiated field terms from each transmitting group to each receiving group elsewhere on the surface. This translation operator is diagonal; there is no interaction between field components propagating in different directions. This is the key to the efficiency of the FMM.

Finally, the received radiation pattern at each group is transformed by the summation over $l' \notin B_l$ and the integration into the spatial domain fields on the surface of the scatterer. Normally in the 2-level FMM, the group size M is chosen to be $M \sim \sqrt{N}$, where N is the total number of surface current unknowns. The resulting cost of a matrix-vector multiply is $O(N^{3/2})$ instead of the N^2 operations required for a dense matrix-vector multiply. Since for each current basis, BM matrix elements and $2K$ multipole expansion coefficients should be calculated and stored before solving the equation iteratively, where B is the average number of near groups. Therefore, memory usage for this algorithm is also $O(N^{3/2})$.

One possibility to further accelerate this algorithm is to implement a multi-level version of the FMM, in which the scatterer is subdivided recursively into smaller and smaller groups, and the FMM is applied in a nested manner. This method, called the multi-level fast multipole algorithm (MLFMA), has been implemented previously by several researchers [49], [54]-[55]. This method reduces the cost of a matrix-vector multiply, and the associated memory usage, to $O(N \log N)$. However, as noted in [49], this algorithm has a higher leading cost constant than the 2-level FMM, so CPU time savings may not be realized for problems of moderate size. However, as will be seen below, the memory savings of the MLFMA are substantial.

The new algorithm developed here is based on the FMM, and is designed to take advantage of the nearly planar geometry of the rough surface. The main idea is the following: choose the group size M to be a small constant, independent of the problem size (the number of groups is thus proportional to

N), and place the FMM group centers on a regular three-dimensional lattice. Then the discretized translation operator $\mathbf{T}$ becomes convolutional and may be applied in $O(N \log N)$ operations using the FFT.

Mathematically, the translation operation required to compute a matrix-vector multiply may be written as [45]

$$\mathbf{g}_l(\hat{k}) = \sum_{l' \notin B_l} T_{ll'}(\hat{k} \cdot \mathbf{r}_{ll'}) \mathbf{s}_{l'}(\hat{k}). \tag{23}$$

In the above equation, $\mathbf{s}_{l'}(\hat{k}) = \sum_{n \in G_{l'}} \mathbf{V}^*_{sl'n}(\hat{k}) j_n$ is the far-field radiation pattern of group l', tabulated at K directions $\hat{k}$ (recall that $K \sim M$, a constant). The quantity $\mathbf{g}_l(\hat{k})$ is the received field pattern at group l, and must be computed for all l and for all discrete propagation directions $\hat{k}$.

If the group centers are constrained to lie on a regular three-dimensional lattice, then l and l' can be represented by three discrete indices corresponding to points in the lattice, say $l = (i, j, k)$ and $l' = (i', j', k')$. Then $\mathbf{r}_{ll'}$ takes the form $\mathbf{r}_{l-l'}$ or, more explicitly, $\mathbf{r}_{(i-i', j-j', k-k')}$. Therefore, the translation operator $\mathbf{T}$ takes the same form, $T_{ll'} = T_{(i-i', j-j', k-k')}$. For a single value of propagation direction $\hat{k}$, Equation (23) may, therefore, be evaluated using a three-dimensional FFT, at a cost proportional to $N_{3D} \log(N_{3D})$, where N_{3D} is the total number of points in the three-dimensional lattice. For a rough-surface problem with fixed RMS surface height, the thickness of the grid in the z direction will not grow with increasing (transverse) problem size but will remain constant. In this case, N_{3D} will be proportional to N, the number of surface current unknowns. Because the translation must be carried out for each value of $\hat{k}$, the total work required to apply $\mathbf{T}$ is proportional to $KN \log N$. Because K is independent of N in this scheme, the computational complexity of applying $\mathbf{T}$ is $O(N \log N)$. Furthermore, since $\mathbf{T}$ is convolutional, only $O(N)$ memory is needed to store the operator matrix.

As discussed above, calculating contributions from near groups, multipole expansion coefficients, all need $O(NM)$ operations. Because M is independent of N in this scheme, all of these calculations may thus be needed in $O(N)$ operations. Therefore, the total complexity of a matrix-vector multiply using this FMM-FFT algorithm is $O(N \log N)$. The memory requirement of this solution strategy is of $O(N)$.

There are several observations that may be made about the FMM-FFT algorithm at this point. Figure 2 illustrates the grouping strategies used by

FMM

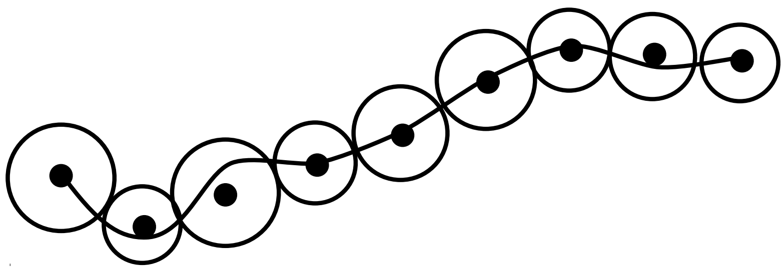

FMM-FFT

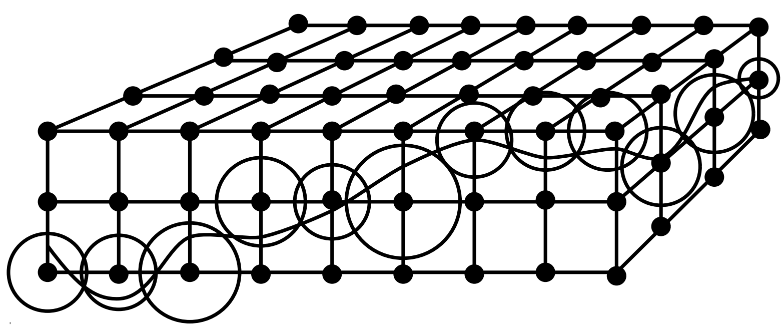

Figure 2. Illustration of the different grouping strategies employed by the FMM and FMM-FFT methods. In the FMM, the locations of the group centers are chosen to minimize the diameter of each group. In the FMM-FFT, the group centers are constrained to lie on a regular three-dimensional lattice.

the FMM and the FMM-FFT. One cost of forcing the group centers to lie on a regular grid is that, in general, the diameter of each group will be slightly larger than in the original FMM, where the group centers are chosen to minimize the group diameter. This increase in group diameter has the effect of increasing K, the number of propagation directions needed in the FMM field expansion. Recall that K is related to the maximum group diameter, D, by the expression $K = 2(k_0 D + \ln(k_0 D + \pi))^2$. To minimize this effect, the grid spacing in the z direction is chosen to be the same as in the x and y directions. For small roughness, the group centers are constrained to lie on $z = 0$ plane. The transverse grid spacing is determined by the size of the FMM groups used in modeling the rough surface.

Also, there is some inefficiency in the FMM-FFT algorithm due to the fact that the original problem, in which the unknowns are arranged on a two-dimensional surface, has now been embedded in a three-dimensional grid. This procedure has the effect of making N_{3D}, the number of grid points in the three-dimensional lattice, significantly larger than the number of FMM groups. This effect is clearly larger for surfaces with greater RMS surface height σ. However, the method is valid (i.e., will produce correct results) for *any* roughness parameters. Note that the radiation function $s_{(i',j',k')}(\hat{k})$ is simply set to zero for each grid point that does not have an associated FMM current group, so the calculation of Equation (23) by FFT convolution does not contain any non-physical sources.

Furthermore, since the translation operation is a linear convolution, the grid data must be zero padded by a factor of two in each spatial dimension to avoid unwanted edge effects due to the circular convolution computed via FFT. For a three-dimensional grid, this zero padding increases the effective FFT size by a factor of eight.

Despite these potential difficulties, the method still offers the possibility of very efficient calculation for the rough-surface scattering problem, especially for surfaces that have moderate RMS surface height. As noted above, however, the method is applicable to surfaces with arbitrary roughness parameters. It is hoped, because of the relative simplicity of the FMM-FFT algorithm, that this method may be more efficient for the rough-surface problem than other methods, such as the multi-level FMM, which have comparable computational complexity ($O(N \log N)$).

We note that this algorithm bears some similarity to other computational electromagnetics algorithms that have been proposed. For example, this algorithm is similar to the CG-FFT algorithm [57]-[59], the FFT T-matrix method of Chew et al. [60], the "canonical grid" methods of Tsang et al. [27], Pak et al. [34], and Chan and Tsang [61], and the AIM method of Bleszynski et al. [62]. In particular, the methods in [34] and [62] are quite similar in that they attack the surface scattering problem by mapping the currents onto a regular grid then applying the FFT to speed the field computations. The difference between these methods and the FMM-FFT method proposed here is in the way the currents are mapped onto a regular grid. In the AIM [62], the physical currents are represented by properly weighted point sources located on a regular three-dimensional grid. In the SMFSIA method [34], the rough-surface problem is mapped onto a regular two-dimensional grid using a Taylor series expansion of the Green's function. In the FMM-FFT, the currents are mapped to a regular three-dimensional grid using the FMM plane-wave field expansion.

5. Numerical Results

As an initial test case, consider a Gaussian rough surface with edge length $L = 9.15\lambda$, RMS surface height $\sigma = 0.1\lambda$, and transverse correlation length $l = 1.0\lambda$. The incident field is a normally incident plane wave, polarized in the x direction. The problem was discretized with seven unknowns per wavelength in the x-y plane (i.e., $\triangle = \lambda/7$, where $\triangle$ is the discretization length in the x-y plane) for a total of $N = 8,064$ surface current unknowns. The conjugate-gradient solution was stopped at a relative residual error of 10^{-3}, requiring a total of 76 CG iterations. The geometry and scattered field are shown in Figure 3. As seen, the radar cross section (RCS) results obtained using the FMM and the FMM-FFT overlay one another exactly. The FMM code used to generate these results is the single-stage code described in detail in [52]. This code also served as the starting point for developing the FMM-FFT code used here.

The computational requirements for each method are summarized in Table 1. These simulations were carried out on a SUN SPARC-10 workstation with 128 MB of RAM. The computational requirements for the multi-level fast-multipole algorithm (MLFMA) are also shown here. The MLFMA code

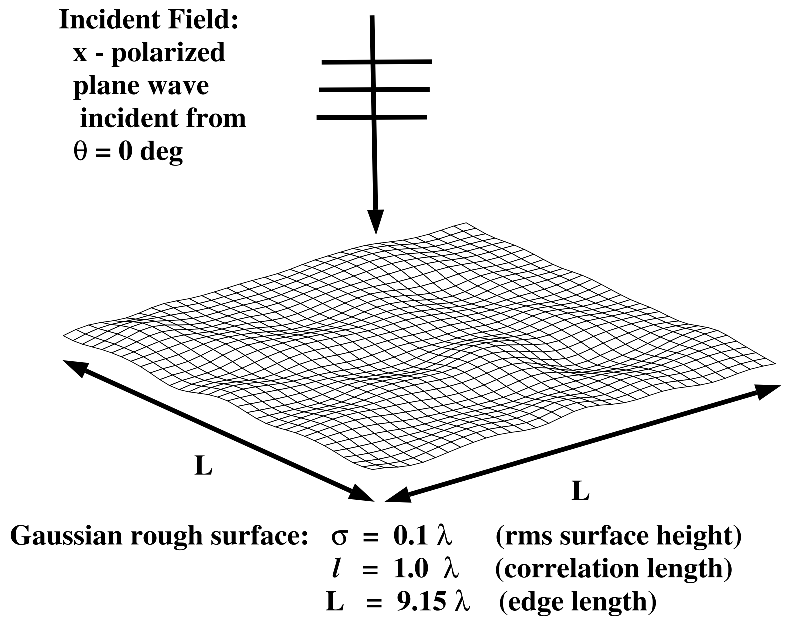

(a)

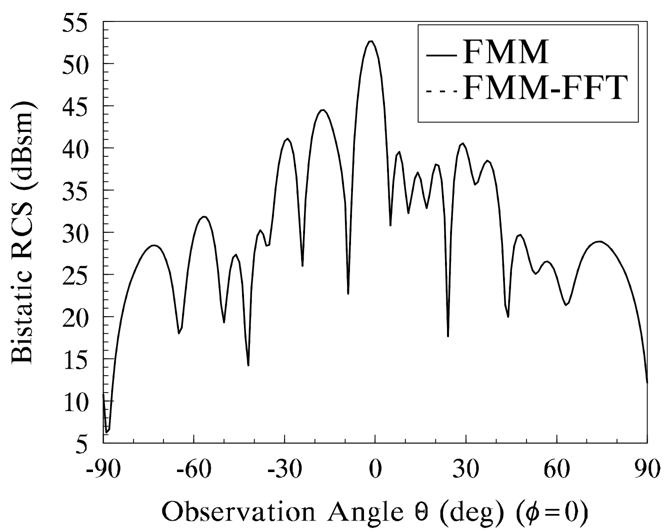

(b)

Figure 3. A test case comparing the FMM and the FMM-FFT. The geometry is shown in (a), the results in (b). The results overlay one another.

used to generate the results of this paper is described in detail in [54]. Note that the results for the standard MOM are estimated, as the memory requirements for this approach exceed the capacity of the workstation used. For the FMM and the FMM-FFT methods, the rough surface was divided into an array of sixteen by sixteen groups, with four unknowns along the edge of each group. Thus, the FMM-FFT lattice spacing for this problem was $4\lambda/7$. Because the roughness is small for this problem, the FMM-FFT group centers were all constrained to lie in the $z = 0$ plane. The number of plane waves used in the field expansion for both the FMM and the FMM-FFT was $K = 128$. (Note that the MLFMA requires a slightly different surface description. For the MLFMA, one current unknown is assigned to each edge of every parametric patch. Thus, a different randomly generated surface with the same roughness parameters was used to test this code.) Clearly, the FMM based methods show vastly improved performance compared with a standard MOM approach. The FMM-FFT shows the best performance of all of the methods for this test case, with a total solution time of 82 min. Note, however, that the MLFMA displays two advantages over the other methods listed: smaller memory usage and reduced fill time.

Table 1. Computational requirements for the test case shown in Figure 3. Times are for a SUN SPARC-10 workstation with 128 MB RAM. ($\sigma = 0.1\lambda$, $l = 1.0\lambda$, $L = 9.15\lambda$, $\triangle = \lambda/7$, $N = 8,064$, $\text{CGTOL} = 10^{-3}$)

Method	Memory	Fill	Solve (76 CG iter)	Mat-Vec
FMM-FFT	80 MB	48 min	34 min	13.5 sec
FMM	177 MB	54 min	92 min	36 sec
MLFMA	27 MB	12 min	109 min	43 sec
MOM*	520 MB	12 hr	5 hr	120 sec

* estimated

The computational requirements are larger for rougher surfaces. The brute-force MOM, the single-stage FMM, and the FMM-FFT all require more than 128 MB of RAM for the case $\sigma = 0.7\lambda$, $l = 1.5\lambda$. These roughness parameters were chosen as good candidates for producing backscattering enhancement, based on the data presented by Ishimaru [2]. The RMS slope for this surface is $\sqrt{2}\sigma/l = 0.66$. The difficulty with this case stems from the fact that increasing the RMS slope increases the area of the rough surface.

Thus, each basis function covers a larger area, and the electrical size of the FMM groups increases. This means that a larger number of plane waves, K, must be used in the FMM field expansion. The alternative is to increase the number of FMM groups (making each group smaller). Either approach has the effect of increasing the memory requirements for the problem.

To circumvent this difficulty, we have used the MLFMA. The computer resources required to implement the MLFMA for the case $\sigma = 0.7\lambda$, $l = 1.5\lambda$ are summarized in Table 2. All parameters, except the surface roughness, are the same as for the previous example. As noted above, several facts stand out about the MLFMA. First, the memory required for the MLFMA is only 30 MB, significantly less than any of the other methods shown in Table 1. Second, the matrix fill time for the MLFMA is 11 min, again much less than for the other methods. The time for a matrix-vector multiply for this problem using the MLFMA is 82 sec, which is less time than is required by the brute-force MOM approach. Thus, the MLFMA is the only one of the computer codes discussed here that is suitable for modeling large-scale rough surfaces in the backscattering enhancement regime, using a typical engineering workstation.

Table 2. Computational requirements for a test case similar to that shown in Figure 3 but with roughness parameters $\sigma = 0.7\lambda$, $l = 1.5\lambda$. Times are for a SUN SPARC-10 workstation with 128 MB RAM. ($L = 9.15\lambda$, $\triangle = \lambda/7$, $N = 8,064$, CGTOL $= 10^{-3}$)

Method	Memory	Fill	Solve (146 CG iter)	Mat-Vec
MLFMA	30 MB	11 min	6.65 hr	82 sec

The total solution time using the MLFMA, however, is still fairly large due to the large number of CG iterations (146) needed to achieve a relative residual error of 10^{-3}. The CG iteration converges more slowly for rougher surfaces, which is consistent with the findings of other researchers. For example, Devayya and Wingham [23] observed that the rate of convergence of the CG method applied to a one-dimensional rough surface is proportional to the RMS surface slope. Tran and Maradudin [33] note that the Neumann-Liouville iterative method stops converging when the RMS slope is approximately one. When the surface becomes rougher, more multiple scattering terms have contributions to the total scattered field. So, the CG iteration converges more slowly for rougher surfaces. EFIE (9) is the first kind of integral equations. Its diagonal elements are less dominant than the second kind of integral equations, such as magnetic field integral equation (MFIE). But it can be applied to both open and closed objects.

In order to reduce the total solution time, we investigated the effects of relaxing the CG convergence condition. The results are shown in Figure 4. The RCS is plotted for the case of a vertically polarized Gaussian beam of half-width $W = 2.3\lambda$ incident from $(\theta = 10^\circ, \phi = 0^\circ)$. The CG iteration is stopped when the following condition is satisfied

$$\frac{||\mathbf{Z} \cdot \mathbf{j}_{comp} - \mathbf{e}||}{||\mathbf{e}||} < \text{CGTOL}, \tag{24}$$

where $\mathbf{j}_{comp}$ is the approximate surface current vector computed by the CG method, and CGTOL is the solution tolerance. As seen, increasing CGTOL from 10^{-3} to 10^{-1} has little effect on the RCS. However, the number of CG iterations required drops from 146 for CGTOL $= 10^{-3}$ to only 31 for CGTOL $= 10^{-1}$. Considering that the results will be statistically averaged in a Monte Carlo simulation, it appears that little information will be lost by relaxing the convergence condition. Thus, CGTOL $= 10^{-1}$ is used to generate the Monte Carlo results presented below.

The Monte Carlo simulations presented in this section were run on an HP9000/715/50 workstation with 64 MB of RAM. This workstation performs at approximately 18 Mflop/sec. This performance is faster than that for the SUN SPARC-10 workstation used for the code development and testing, which performs at approximately 10 Mflop/sec. (An extensive listing of the performance of different computer systems is available from the *netlib* repository at Oak Ridge National Laboratory. This database can be accessed on the World Wide Web at the address "http://www.netlib.org/index.html".)

The first Monte Carlo simulation was performed using rough-surface parameters $\sigma = 0.7\lambda$, $l = 1.5\lambda$, $L = 9.15\lambda$, $\triangle = \lambda/7$, and $N = 8,064$. The incident field is a vertically polarized Gaussian beam of half-width $W = 2.3\lambda$ incident from $(\theta = 10^\circ, \phi = 0^\circ)$. The MLFMA program was used to calculate the scattering from a total of 100 randomly generated rough surfaces. On the HP9000/715/50 workstation, the matrix fill time for each surface was 6 min,

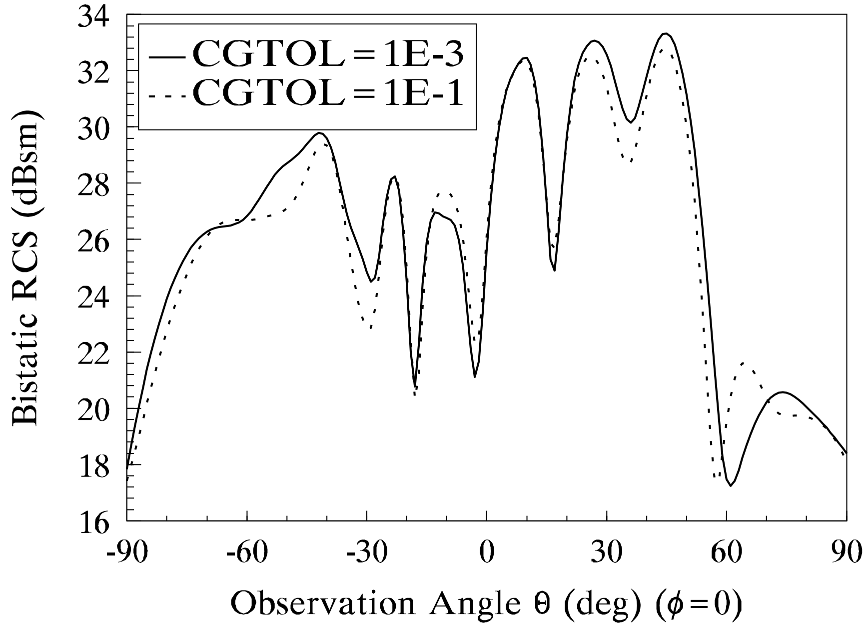

Figure 4. The effects on the RCS of changing the CG convergence criterion, CGTOL. In this case, the MLFMA is used to compute the scattering from a rough surface with parameters $\sigma = 0.7\lambda$ and $l = 1.5\lambda$, $L = 9.15\lambda$, $\triangle = \lambda/7$, $N = 8,064$.

and the average solve time was 41 min; an average of 27 CG iterations were required to achieve a relative residual error of CGTOL $= 10^{-1}$. Thus, the total simulation time was 100×47 min $= 78$ hr of CPU time. The program used 30 MB of memory.

The results of the first Monte Carlo simulation are shown in Figure 5. There is a pronounced peak of the scattering coefficient in the backscattering direction, $(\theta = 10^\circ, \phi = 0^\circ)$. This backscattering enhancement effect is quite strong in both the co-polarized scattering (VV) and the cross-polarized (HV) scattering. This result contrasts strongly with the second Monte Carlo simulation, discussed below.

The second Monte Carlo simulation carried out was run on the same set of 100 surfaces used in the first simulation, but with the surface height reduced by a factor of ten. Thus, the surface roughness parameters for the second simulation were $\sigma = 0.07\lambda$ and $l = 1.5\lambda$. The results of this simulation, along with the results of the approximate analytical Kirchhoff theory [3], are shown in Figure 6. There is excellent agreement between the two solution methods, as should be the case for this relatively smooth surface. The behavior of the scattering coefficient is very different than for the rougher surface of the first simulation. In this case, the incoherent field intensity is spread out in a cone centered around the specular direction. For the rougher surface, the incoherent intensity is quite diffuse, with a peak in the backscattering direction.

A word is in order concerning the statistical significance of these Monte Carlo simulations. Recall that the bistatic scattering coefficient, γ, is proportional to the statistical variance of the scattered electric field computed over the set of surface realizations. Let γ_n denote the scattering coefficient computed from a Monte Carlo simulation with n random surfaces, and let γ_{true} denote the true value of γ. Note that γ_n is itself a random variable that depends upon the n sample surfaces used in the Monte Carlo simulation. Assuming that the scattered field follows a Gaussian probability distribution, the standard deviation of γ_n, and hence the expected error due to statistical sampling, is equal to $\sqrt{\frac{2}{n-1}}\gamma_{\text{true}}$ [63]. For $n = 100$ samples, this standard deviation is equal to $0.14\gamma_{\text{true}}$. Alternatively, the 90% confidence interval for γ is given by $\left((n-1)\gamma_n/\chi^2_{0.05,n-1}, (n-1)\gamma_n/\chi^2_{0.95,n-1}\right)$, where $\chi^2_{\alpha,n-1}$ is the chi-square probability distribution with $n-1$ degrees of freedom [63]. Eval-

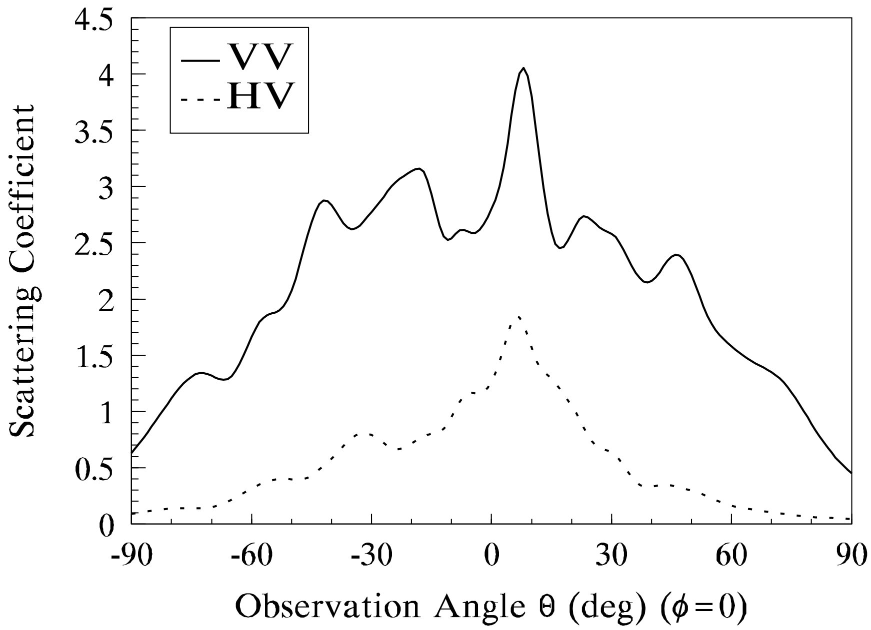

Figure 5. Monte Carlo simulation of the bistatic scattering coefficient γ for a rough surface with RMS height $\sigma = 0.7\lambda$ and transverse correlation length $l = 1.5\lambda$. The angle of incidence is $(\theta = 10^\circ, \phi = 0^\circ)$.

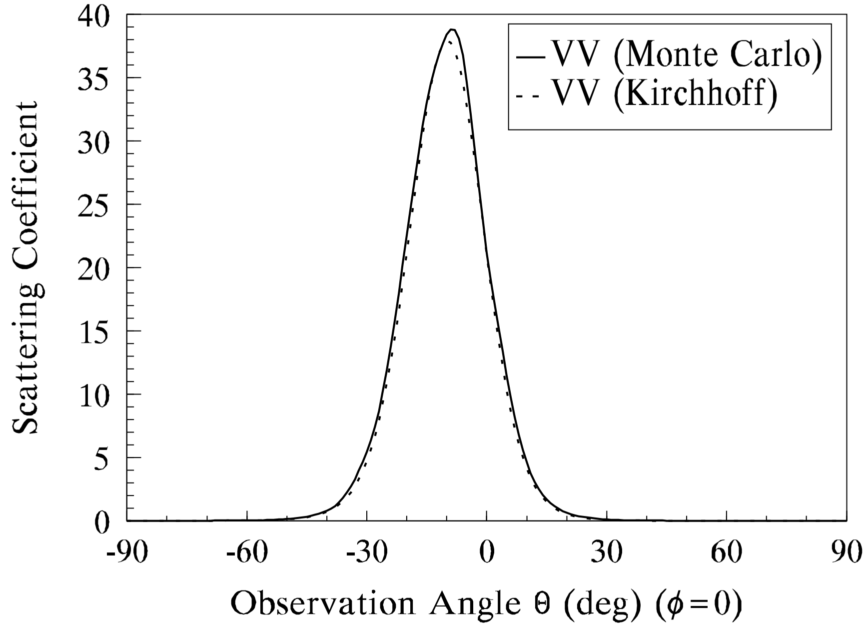

Figure 6. Monte Carlo simulation of the bistatic scattering coefficient γ for a rough surface with RMS height $\sigma = 0.07\lambda$ and transverse correlation length $l = 1.5\lambda$. The angle of incidence is $(\theta = 10^{\circ}, \phi = 0^{\circ})$. Also shown are the results of the Kirchhoff theory.

uating the above expression for $n = 100$ samples, we find that there is a 90% probability that γ_{true} lies in the range $(0.80\gamma_{100}, 1.28\gamma_{100})$. This statement holds true for each observation angle.

Finally, we wish to investigate further the performance of the FMM-FFT algorithm for the case of large-scale rough-surface problems. As noted previously, this algorithm was not used for the Monte Carlo simulations above (with roughness parameters $\sigma = 0.7\lambda$ and $l = 1.5\lambda$) because the memory requirements for the FMM-FFT code exceeded the memory available on the computer workstations used for the simulations.

To generate the following results, we made use of a larger computer, a Silicon Graphics Inc. (SGI) Power Challenge operated by the National Center for Supercomputing Applications (NCSA) at the University of Illinois at Urbana-Champaign. The Power Challenge is a parallel machine with sixteen processors and 4 GB of shared memory. Each processor has a theoretical peak speed of 300 Mflop/sec. ¿From the *netlib* performance database, the actual single processor speed, based on a standard linear algebra benchmark, is 104 Mflop/sec. A single processor of the Power Challenge was used for the following calculations.

Both the FMM-FFT and the MLFMA were run for a series of test cases with surface parameters $l = 1.5\lambda$, $L = 9.15\lambda$, $\triangle = \lambda/7$, and $N = 8,064$. The RMS surface height σ was varied. The results are shown in Table 3. The column labeled N_z is the number of z-levels in the three-dimensional FMM-FFT lattice. Not shown in the table is the matrix fill time; the FMM-FFT fill required 16 min, independent of σ, while the MLFMA fill required 2.7 min, also independent of σ. (For both of these algorithms the fill time is dominated by the near-neighbor fill time, which is independent of σ.) In terms of the time required for one matrix-vector multiply, the FMM-FFT outperforms the MLFMA for the two smoother surfaces. For the rougher surfaces, the MLFMA displays superior performance, which is consistent with the theoretical discussion of the performance of the FMM-FFT presented in Section 4.

6. Conclusions

In this paper, we have addressed the challenging goal of solving large-scale random rough-surface scattering problems using an MOM/Monte Carlo

Table 3. Comparison of the performance of the FMM-FFT and MLFMA for computing the scattering from a large-scale rough surface. Times are for a single processor of an SGI Power Challenge supercomputer. N_z is the number of z-levels in the three-dimensional FMM-FFT lattice. ($l = 1.5\lambda$, $L = 9.15\lambda$, $\triangle = \lambda/7$, $N = 8,064$)

RMS Height σ	N_z	Memory FMM-FFT	Memory MLFMA	Mat-Vec FMM-FFT	Mat-Vec MLFMA
0.07λ	1	81 MB	30 MB	1.0 sec	7.0 sec
0.12λ	2	104 MB	30 MB	4.9 sec	7.5 sec
0.35λ	4	194 MB	30 MB	13.0 sec	9.0 sec
0.7λ	8	251 MB	30 MB	18.9 sec	11.4 sec

approach combined with efficient computational strategies.

A new FMM-FFT algorithm has been developed and investigated. This algorithm requires $O(N)$ memory and $O(N \log N)$ CPU time per matrix-vector multiply. The resulting computer code has been shown to be very efficient for surfaces with small RMS surface height, outperforming other fast algorithms such as the FMM and the MLFMA. While the FMM-FFT is most efficient for small-scale roughness, the algorithm is also applicable to problems with large-scale roughness. An advantage of the FMM-FFT is the relatively simple structure of the algorithm. Since much of the computational burden is placed on the calculation of FFTs, machine-specific subroutine libraries can be used to implement the algorithm efficiently.

For problems with larger RMS surface heights, the MLFMA was found to provide superior performance. The main advantages of the MLFMA are its small memory usage and moderate matrix fill time. The algorithm requires $O(N \log N)$ memory and $O(N \log N)$ CPU time per matrix-vector multiply.

Using the MLFMA, Monte Carlo simulations have been performed to compute the scattering of three-dimensional vector electromagnetic waves from two-dimensional perfectly conducting random rough surfaces. The simulations were carried out on a set of 100 Gaussian rough surfaces with edge length $L = 9.15\lambda$ and discretization length $\triangle = \lambda/7$, for a total of $N = 8,064$ surface current unknowns. The roughest surface considered had RMS surface height $\sigma = 0.7\lambda$ and transverse correlation length $l = 1.5\lambda$. Computations were also performed for a smoother surface with $\sigma = 0.07\lambda$ and $l = 1.5\lambda$. For the rougher surface, the total Monte Carlo simulation time (for all 100 rough surface realizations) was 78 hr, using an HP9000/715/50 workstation. The program used 30 MB of memory.

For the rougher surface, backscattering enhancement is clearly observable as a pronounced peak, in the backscattering direction, of the computed bistatic scattering coefficient. The field behavior is quite different for the smoother surface, where the incoherent field intensity is spread out in a cone centered around the specular direction. For the smoother surface, the Monte Carlo results compare well with the results of the approximate Kirchhoff theory.

References

[1] A. Ishimaru, "Experimental and theoretical studies on enhanced backscattering from scatterers and rough surfaces," in *Scattering in Volumes and Surfaces*, M. Nieto-Vesperinas and J. C. Dainty, Eds. Amsterdam: North-Holland, pp. 1-15, 1990.

[2] A. Ishimaru, "Backscattering enhancement: from radar cross sections to electron and light localizations to rough-surface scattering," *IEEE Antennas Propagat. Mag.*, vol. 33, no. 5, pp. 7-11, October 1991.

[3] J. A. Kong, *Electromagnetic Wave Theory.* New York: Wiley, 1986.

[4] S. O. Rice, "Reflection of electromagnetic waves from slightly rough surfaces," *Commun. Pure Appl. Math.*, vol. 4, pp. 351-378, 1951.

[5] G. R. Valenzuela, "Depolarization of EM waves by slightly rounded surfaces," *IEEE Trans. Antennas Propagat.*, vol. 15, pp. 552-557, 1967.

[6] J. C. Leader, "Bidirectional scattering of electromagnetic waves from rough surfaces," *J. Appl. Phys.*, vol. 42, no. 12, pp. 4808-4816, November 1971.

[7] E. Bahar and B. S. Lee, "Full wave solutions for rough-surface bistatic radar cross sections: comparison with small perturbation, physical optics, numerical, and experimental results," *Radio Science*, vol. 29, no. 2, pp. 407-429, March-April 1994.

[8] R. E. Collin, "Electromagnetic scattering from perfectly conducting rough surfaces (a new full wave method)," *IEEE Trans. Antennas Propagat.*, vol. 40, no. 12, pp. 1466-1477, December 1992.

[9] R. E. Collin, "Scattering of an incident Gaussian beam by a perfectly conducting rough surface," *IEEE Trans. Antennas Propagat.*, vol. 42, no. 1, pp. 70-74, January 1994.

[10] V. Celli, A. A. Maradudin, A. M. Marvin, and A. R. McGurn, "Some aspects of light scattering from a randomly rough metal surface," *J. Opt. Soc. Am. A*, vol. 2, no. 12, pp. 2225-2239, December 1985.

[11] A. R. McGurn and A. A. Maradudin, "Localization effects in the elastic scattering of light from a randomly rough surface," *J. Opt. Soc. Am. B*, vol. 4, no. 6, pp. 910-926, June 1987.

[12] P. Tran, A. A. Maradudin, and V. Celli, "Backscattering enhancement from a dielectric surface," *J. Opt. Soc. Am. B*, vol. 8, no. 7, pp. 1526-1530, July 1991.

[13] A. A. Maradudin, J. Q. Lu, P. Tran, R. F. Wallis, V. Celli, Z. H. Gu, A. R. McGurn, E. R. Méndez, T. Michel, M. Nieto-Vesperinas, J. C. Dainty,

and A. J. Sant, " Enhanced backscattering from one- and two-dimensional random surfaces," *Revista Mexicana de Física*, vol. 38, no. 3, pp. 343-397, 1992.

[14] A. A. Maradudin and E. R. Méndez, "Enhanced backscattering of light from weakly rough, random metal surfaces," *Appl. Opt.*, vol. 32, no. 19, pp. 3335-3343, July 1993.

[15] K. A. O'Donnell and E. R. Méndez, "Experimental study of scattering from characterized random surfaces," *J. Opt. Soc. Am. A*, vol. 4, no. 7, pp. 1194-1205, July 1987.

[16] E. R. Méndez and K. A. O'Donnell, "Scattering experiments with smoothly varying random rough surfaces and their interpretation," in *Scattering in Volumes and Surfaces*, M. Nieto-Vesperinas and J. C. Dainty, Eds. Amsterdam: North-Holland, pp. 125-141, 1990.

[17] M. E. Knotts and K. A. O'Donnell, "Measurements of light scattering by a series of conducting surfaces with one-dimensional roughness," *J. Opt. Soc. Am. A*, vol. 11, no. 2, pp. 697-710, February 1994.

[18] J. C. Dainty, M. -J. Kim, and A. J. Sant, "Measurements of angular scattering by randomly rough metal and dielectric surfaces," in *Scattering in Volumes and Surfaces*, M. Nieto-Vesperinas and J. C. Dainty, Eds. Amsterdam: North-Holland, pp. 143-155, 1990.

[19] Y. Kuga, J. S. Colburn, and P. Phu, "Millimeter-wave scattering from one-dimensional random rough surfaces of different surface correlation functions," *Waves in Random Media*, vol. 3, pp. 101-110, 1993.

[20] J. T. Johnson, L. Tsang, R. T. Shin, K. Pak, C. H. Chan, A. Ishimaru, and Y. Kuga, "Backscattering enhancement of electromagnetic waves from two-dimensional perfectly conducting random rough surfaces: A comparison of Monte Carlo simulations with experimental data," *IEEE Trans. Antennas Propagat.*, vol. 44, no. 5, pp. 748-756, May 1996.

[21] R. Axeline and A. K. Fung, "Numerical computation of scattering from a perfectly conducting random surface," *IEEE Trans. Antennas Propagat.*, vol. 26, pp. 482-488, May 1978.

[22] N. Garcia and E. Stoll, "Monte Carlo calculation for electromagnetic-wave scattering from random rough surfaces," *Phys. Rev. Lett.*, vol. 52, no. 20, pp. 1798-1801, May 1984.

[23] R. Devayya and D. J. Wingham, "The numerical calculation of rough-surface scattering by the conjugate gradient method," *IEEE Geosci. Remote Sensing*, vol. 30, no. 3, pp. 645-648, May 1992.

[24] L. Tsang, C. H. Chan, H. Sangani, A. Ishimaru, and P. Phu, "A banded matrix iterative approach to Monte Carlo simulations of large-scale random rough-surface scattering: TE case," *J. Electromagn. Waves and Appl.*, vol. 7, no. 9, pp. 1185-1200, 1993.

[25] L. Tsang, C. H. Chan, K. Pak, H. Sangani, A. Ishimaru and P. Phu, "Monte Carlo simulations of large-scale composite random rough-surface scattering based on the banded-matrix iterative approach," *J. Opt. Soc. Am. A*, vol. 11, no. 2, pp. 691-696, February 1994.

[26] L. Li, C. H. Chan, L. Tsang, K. Pak, and P. Phu, "Monte Carlo simulations and backscattering enhancement of random metallic rough surfaces at optical frequencies," *J. Electromagn. Waves and Appl.*, vol. 8, no. 3, pp. 277-293, 1994.

[27] L. Tsang, C. H. Chan, K. Pak, and H. Sangani, "Monte-Carlo simulations of large-scale problems of random rough-surface scattering and applications to grazing incidence with the BMIA/canonical grid method," *IEEE*

Trans. Antennas Propagat., vol. 43, no. 8, pp. 851-859, August 1995.

[28] P. Tran and A. A. Maradudin, "Scattering of a scalar beam from a two-dimensional randomly rough hard wall: enhanced backscattering," *Phys. Rev. B*, vol. 45, no. 7, pp. 3936-3939, February 1992.

[29] P. Tran and A. A. Maradudin, "Scattering of a scalar beam from a two-dimensional randomly rough hard wall: Dirichlet and Neumann boundary conditions," *Appl. Opt.*, vol. 32, no. 15, pp. 2848-2851, May 1993.

[30] L. Tsang, C. H. Chan, and K. Pak, "Monte Carlo simulation of a two-dimensional random rough surface using the sparse-matrix flat-surface iterative approach," *Electron. Lett.*, vol. 29, no. 13, pp. 1153-1154, June 1993.

[31] L. Tsang, C. H. Chan, and K. Pak, "Backscattering enhancement of a two-dimensional, random rough surface (three-dimensional scattering) based on Monte Carlo simulations," *J. Opt. Soc. Am. A*, vol. 11, no. 2, pp. 711-715, February 1994.

[32] P. Tran, V. Celli, and A. A. Maradudin, "Electromagnetic scattering from a two-dimensional randomly rough, perfectly conducting surface: iterative methods," *J. Opt. Soc. Am. A*, vol. 11, no. 5, pp. 1686-1689, May 1994.

[33] P. Tran and A. A. Maradudin, "The scattering of electromagnetic waves from a randomly rough 2D metallic surface," *Opt. Commun.*, vol. 110, pp. 269-273, August 15, 1994.

[34] K. Pak, C. H. Chan, and L. Tsang, "A SMFSIA method for the electromagnetic scattering from a two-dimensional (3-D scattering problem) perfectly conducting random rough surface," *IEEE APS Int. Symp. Dig.*, pp. 451-454, June 1994.

[35] A. K. Fung, M. R. Shah, and S. Tjuatja, "Numerical simulation of scattering from three-dimensional randomly rough surfaces," *IEEE Geosci. Remote Sensing*, vol. 32, no. 5, pp. 986-994, September 1994.

[36] W. C. Chew, *Waves and Fields in Inhomogeneous Media.* New York: Van Nostrand Reinhold, 1990.

[37] E. Burstein, A. Hartstein, J. Schoenwald, A. A. Maradudin, D. L. Mills, and R. F. Wallis, "Surface polaritons - electromagnetic waves at interfaces," in *Polaritons*, E. Burstein and F. de Martini, Eds. London: Pergamon, pp. 89-108, 1974.

[38] D. Maystre and M. Saillard, "Localization of light by randomly rough surfaces: concept of localiton," *J. Opt. Soc. Am. A*, vol. 11, no. 2, pp. 680-690, February 1994.

[39] J. M. Song and W. C. Chew, "Moment method solutions using parametric geometry," *J. Electromagn. Waves and Appl.*, vol. 9, no. 1/2, pp. 71-83, 1995.

[40] S. Wandzura, "Electric current basis functions for curved surfaces," *Electromagn.*, vol. 12, pp. 77-91, 1992.

[41] S. M. Rao, D. R. Wilton, and A. W. Glisson, "Electromagnetic scattering by surfaces of arbitrary shape," *IEEE Trans. Antennas Propagat.*, vol. 30, no. 3, pp. 409-418, May 1982.

[42] V. Rokhlin, "Rapid solution of integral equations of scattering theory in two dimensions," *J. Comput. Phys.*, vol. 36, no. 2, pp. 414-439, February 1990.

[43] N. Engheta, W. D. Murphy, V. Rokhlin, and M. S. Vassiliou, "The fast multipole method (FMM) for electromagnetic scattering problems," *IEEE Trans. Antennas Propagat.*, vol. 40, no. 6, pp. 634-641, June 1992.

[44] V. Rokhlin, "Diagonal forms of translation operators for the Helmholtz equation," *Applied and Computational Harmonic Analysis*, vol. 1, pp. 82-93, 1993.

[45] R. Coifman, V. Rokhlin, and S. Wandzura, "The fast multipole method for the wave equation: a pedestrian prescription," *IEEE Antennas Propagat. Mag.*, vol. 35, no. 3, pp. 7-12, June 1993.

[46] L. R. Hamilton, M. A. Stalzer, R. S. Turley, J. L. Visher, and S. M. Wandzura, "Scattering computation using the fast multipole method," *IEEE APS Int. Symp. Dig.*, pp. 852-855, 1993.

[47] C. C. Lu and W. C. Chew, "Fast algorithm for solving hybrid integral equations," *IEE Proc.-H*, vol. 140, no. 6, pp. 455-460, December 1993.

[48] R. Coifman, V. Rokhlin, and S. Wandzura, "Faster single-stage multipole method for the wave equation," *10th Annual Review of Progress in Applied Computational Electromagnetics*, pp. 19-24, March 1994.

[49] C. C. Lu and W. C. Chew, "A multilevel algorithm for solving boundary integral equations of wave scattering," *Microwave Opt. Technol. Lett.*, vol. 7, no. 10, pp. 466-470, July 1994.

[50] R. L. Wagner and W. C. Chew, "A ray-propagation approach for accelerating the fast multipole method," *IEEE APS Int. Symp. Dig.*, pp. 427-430, June 1994.

[51] R. L. Wagner and W. C. Chew, "A ray-propagation fast multipole algorithm," *Microwave Opt. Technol. Lett.*, vol. 7, no. 10, pp. 435-438, July 1994.

[52] J. M. Song and W. C. Chew, "Fast multipole method solution using parametric geometry," *Microwave Opt. Technol. Lett.*, vol. 7, no. 16, pp. 760-765, November 1994.

[53] J. M. Song and W. C. Chew, "Fast multipole method solution of the combined field integral equation," *11th Annual Review of Progress in Applied Computational Electromagnetics*, pp. 629-636, March 1995.

[54] J. M. Song and W. C. Chew, "Multilevel fast-multipole algorithm for solving combined field integral equations of electromagnetic scattering," *Microwave Opt. Technol. Lett.*, vol. 10, no. 1, pp. 14-19, September 1995.

[55] B. Dembart and E. Yip, "A 3D fast multipole method for electromagnetics with multiple levels," *11th Annual Review of Progress in Applied Computational Electromagnetics*, pp. 621-628, March 1995.

[56] M. A. Epton and B. Dembart, "Multipole translation theory for the three-dimensional Laplace and Helmholtz equations," *SIAM J. Sci. Comput.*, vol. 16, no. 4, pp. 865-897, July 1995.

[57] D. T. Borup and O. P. Gandhi, "Fast-Fourier-transform method for calculation of SAR distributions in finely discretized inhomogeneous models of biological bodies," *IEEE Trans. Microwave Theory Tech.*, vol. 32, no. 4, pp. 355-360, April 1984.

[58] D. T. Borup, D. M. Sullivan, and O. P. Gandhi, "Comparison of the FFT conjugate gradient method and the finite-difference time-domain method for the 2-D absorption problem," *IEEE Trans. Microwave Theory Tech.*, vol. 35, no. 4, April 1987.

[59] C. Shen, K. J. Gover, M. I. Sancer, and A. D. Varvatsis, "The discrete Fourier transform method of solving differential-integral equations in scattering theory," *IEEE Trans. Antennas Propagat.*, vol. 37, no. 8, pp. 1032-1041, August 1989.

[60] W. C. Chew, J. H. Lin, and X. G. Yang, "An FFT T-matrix method for 3D microwave scattering solutions from random discrete scatterers,"

Microwave Opt. Technol. Lett., vol. 9, no. 4, pp. 194-196, July 1995.

[61] C. H. Chan and L. Tsang, “A sparse-matrix canonical-grid method for scattering by many scatterers,” *Microwave Opt. Technol. Lett.*, vol. 8, no. 2, pp. 114-118, February 1995.

[62] E. Bleszynski, M. Bleszynski, and T. Jaroszewicz, “A fast integral-equation solver for electromagnetic scattering problems,” *IEEE APS Int. Symp. Dig.*, pp. 416-419, June 1994.

[63] R. J. Larsen and M. L. Marx, *An Introduction to Mathematical Statistics and its Applications*,” 2nd ed. Englewood Cliffs, NJ: Prentice-Hall, 1986.

List of Figures

List of Talbes